UDK 665.6:628.475
Original scientific article/Izvirni znanstveni članek

ISSN 1580-2949
Mater. Tehnol.

EFFECTS OF A LaNaY CATALYST ON THE PYROLYSIS PRODUCT DUSTRIBUTION AND REACTION MECHANISM OF OIL-PRONE COAL

VPLIVI IN MEHANIZMI La-Na-Y KATALIZATORJA NA PORAZDELITEV PRODUKTOV PIROLIZE PRI IZDELAVI MINERALNEGA OLJA IZ PREMOGA

Qing Ge[1], Gangqiang Zhang[1,2*], Yuge Pang[1], Jing Yang[1]

[1]Xinjiang Xuandong Energy Co., Ltd., Hami, Xinjiang, China
[2]Key Laboratory of Oil and Gas Fine Chemicals, Ministry of Education and Xinjiang Uygur Autonomous Region, School of Chemical Engineering and Technology, Xinjiang University, Urumqi, Xinjiang, China

Prejem rokopisa – received: 2025-06-29; sprejem za objavo – accepted for publication: 2025-10-07

doi:10.17222/mit.2025.1508

Currently, traditional coal pyrolysis processes suffer from low tar yield and poor tar quality, which seriously hinder the development and industrial application of coal pyrolysis technology. To address these challenges, this study innovatively prepares a LaNaY catalyst using ion exchange method and systematically investigates its effect on product distribution during the pyrolysis of oil-prone coal. It designs experiments to optimize the La loading, pyrolysis temperature, and catalyst coal contact method, and investigates the effect of the H_2 atmosphere. The results showed that when the La loading amount was 1.5 *w*/%, the La:Na molar ratio was 1:1, and the catalyst was fully in contact with coal using the in-situ loading method, the tar yield reached a maximum value of 18.6 % at 600 °C under the H_2 atmosphere. At 700 °C, under the same conditions, the H_2/CO molar ratio in the gas product reached 2.5. Compared with traditional NaY molecular sieve catalysts, the introduced La element significantly enhanced the catalytic performance of the LaNaY catalyst. It not only effectively improved the tar yield, but also promoted the generation of light aromatic hydrocarbons by inhibiting heavy polycyclic aromatic hydrocarbons (PAHs), thereby increasing the H/C atomic ratio of tar from 1.2 to 1.5, significantly improving the tar quality. Crucially, the catalyst exhibited high stability over multiple cycles and excellent regenerability, underscoring its potential for industrial application. This study provides an effective solution for an efficient and high-value conversion of oil-prone coal, providing a significant technical foundation for the future optimization of the catalytic pyrolysis technology.

Keywords: oil-prone coal, pyrolysis, Y-molecular sieve, ion exchange

Današnji tradicionalni proces pirolize premoga je problematičen zaradi majhnega izkoristka tvorbe premogovega katrana. To močno ovira njen razvoj in industrijsko uporabo. Zato so avtorji v tem članku opisali inovativno raziskavo, ki opisuje izdelavo in uporabo katalizatorja na osnovi La, Na, in Y z uporabo metode ionske izmenjave. V članku avtorji opisujejo sistematično raziskavo njenega vpliva na porazdelitev produktov med pirolizo ustreznega premoga. V tej študiji so oblikovali eksperimente za optimizacijo nalaganja La, temperaturo pirolize ter metodo stika (kontakta) med katalizatorjem in premogom. Raziskovali so tudi vpliv vodikove (H_2) atmosfere. Rezultati so pokazali, da v primeru molarnega razmerja La:Na 1:1 in 1,5 *w*/ %-ni vsebnosti La, pri popolnem kontaktu s premogom, izkoristek katrana dosega maksimalne vrednosti 18,6% v H_2 atmosferi pri 600 °C. Pri temperaturi pirolize 700 °C in enakih drugih pogojih so dosegli v plinskem produktu molarno razmerje 2,5 med H_2 in CO. Primerjava s tradicionalinim Na-Y katalizatorskim molekularnim sitom je vpeljava La pomembno izboljšala katalitične izkoristek procesa. Ni prišlo samo do učinkovitega povečanja izkoristka katrana temveč je prišlo tudi do tvorbe lahkih aromatičnih ogljikovodikov z zaviranjem tvorbe težkih policikličnih aromatskih ogljikovodikov (PAHs; angl.: heavy polycyclic aromatic hydrocarbons). To je povečalo atomsko razmerje H/C v premogovem katranu z 1,2 na 1,5, kar močno izboljša njegovo kvaliteto. Ključno je, da ima katalizator visoko stabilnost v več ciklih in odlično regenerabilnost, kar poudarja njegov potencial za industrijsko uporabo. V zaključku avtorji članka povdarjajo, da ta študija (raziskava) ponuja rešitve za učinkovito in visokokakovostno pretvorbo premoga, ki je primeren za izdelavo mineralnega olja (nafte), in zagotavlja pomembno tehnično osnovo za prihodnjo optimizacijo tehnologije katalitične pirolize.

Ključne besede: izdelava mineralnega olja iz premoga, piroliza, itrijevo molekularno sito, ionska izmenjava

1 INTRODUCTION

As an important energy and chemical raw material, the clean and efficient utilization of coal has strategic significance for national energy security. Oil-prone coal, a type of low-grade coal, often produces a large amount of low-utilization foam coal during mining, transportation, and use. The hydrogen-rich pyrolysis technology can effectively improve the conversion efficiency and product quality of coal by pyrolyzing it in a hydrogen-rich atmosphere, achieving high-value utilization of low-rank coal, and alleviating the oil shortage.[1] Unlike traditional coal pyrolysis, the H_2 in the hydrogen-rich pyrolysis process can effectively compensate for the low hydrogen-to-carbon ratio of coal itself. By regulating free radical migration and secondary reactions, the yield and quality of tar can be simultaneously improved.[2]

*Corresponding author's e-mail:
GangqiangZz@163.com (Gangqiang Zhang)

Table 1: Experimental instruments and materials

Experimental instruments/equipment/gases	Specification and model	Manufacturer
Box furnace	Avanti J-26 XP	Beckman Coulter International Trading (Shanghai) Co., Ltd
High-speed floor centrifuge	GL21M	Hunan Kaida Scientific Instrument Co., Ltd
Vacuum drying oven	HTCR	Germany Carbolite Gero
Gas chromatography (GC)	GC2030Smart	Shanghai Taitai Ruijie Information Technology Co., Ltd
GC-mass spectrometry (MS)	9100GC-MS	Beijing Leshi Lianchuang Technology Co., Ltd
Brunauer-emmett-teller (BET) analyzer	JW-DX400	Beijing Jingwei Gaobo Instrument Co., Ltd
Scanning electron microscopy (SEM)	Sigma500	Zeiss
Fourier transform infrared spectroscopy (FTIR)	IRSpirit	Shanghai Zhuangrun International Trade Co., Ltd
Inductively coupled plasma-optical emission spectroscopy (ICP-OES)	iCAP 7400	Shanghai Meixi Instrument Co., Ltd
NaY molecular sieve	NKY-5	Beijing Honghaitian Technology Co., Ltd
H_2	Purity 99.99 %	Wuhan Newruide Special Gas Co., Ltd
N_2	Purity 99.999 %	Wuhan Newruide Special Gas Co., Ltd

Molecular sieves, especially Y-type molecular sieves, are widely used in fields such as petroleum catalytic cracking, gas separation, and catalytic reactions due to their unique pore structure, high specific surface area, and controllable acidic sites. A NaY molecular sieve, as a key active component in the preparation of petroleum catalytic cracking catalysts, has been proven to improve reaction activity, selectivity, and stability, thereby enhancing the yield of light oil.[3] In recent years, the application of rare earth elements in the modification of molecular sieve catalysts has received widespread attention. The La element, with its strong Lewis acidity and good ion-exchange ability, can significantly improve the structural stability and selectivity of molecular sieve catalysts for specific reactions. In the process of coal pyrolysis, the La element is expected to optimize the distribution of coal pyrolysis products and improve the tar yield and quality by adjusting the acidity distribution of catalysts.[4]

However, despite the advantages of La and Na in molecular sieve modification, there are only few systematic reports on the synergistic mechanism and performance optimization mechanism of a LaNaY catalyst formed by co-loading La and Na on the Y-molecular sieve during the pyrolysis of oil-prone coal. There is still room for improvement in the tar yield, tar quality (such as the proportion of light components), and high-value-added gas yield in the existing oil-prone coal pyrolysis technology. In addition, the research on the influence of the catalyst-coal contact mode on the selectivity of pyrolysis products is not sufficient. Therefore, this study innovatively prepares a LaNaY catalyst and systematically designs multiple experiments. It aims to achieve the following objectives: (1) Optimizing the preparation conditions and pyrolysis process parameters of a LaNaY catalyst (including La loading, pyrolysis temperature, and atmosphere); (2) Thoroughly investigating the influence of the contact mode between catalyst and coal (physical mixing and in-situ loading) on the pyrolysis product distribution; (3) Revealing the catalytic mechanism of the LaNaY catalyst in improving tar yield, enhancing tar quality (especially inhibiting the polycyclic aromatic hydrocarbons (PAHs) generation), and promoting H_2 yield in oil-prone coal gas. This study is expected to provide theoretical basis and practical guidance for an efficient and high-value conversion of oil-prone coal.

2 METHODS AND MATERIALS

This study successfully prepares a LaNaY catalyst with the ion exchange method and designs a fixed-bed pyrolysis reactor to systematically analyze its effect on the pyrolysis product distribution of oil-prone coal.

2.1 Preparation and optimization of LaNaY catalyst

2.1.1 Experimental instruments and materials

The instruments and materials used in the experiment are shown in **Table 1**. The selected NaY molecular sieve has a relative crystallinity of 90 %, a cell constant of 24.64 μm, a specific surface area of 650 $m^2\ g^{-1}$, and a pore volume of 0.36 mL g^{-1}.

The oil-prone coal powder used in the experiment comes from the Hami Energy Integration Innovation Base project. Its industrial analysis (moisture, ash content, volatile matter, and fixed carbon) is shown in **Table 2**.

Table 2: Industrial analysis of oil-prone coal powder

Component	Content range (*w*/%)	Average value (*w*/%)
Moisture	0.85–9.25	4.91
Ash	5.80–25.20	14.52
Volatile matter	29.26–53.25	41.32
Fixed carbon	35.78–78.61	54.10

The results of elemental analysis (C, H, N, S, and O) of oil-prone coal powder are shown in **Table 3**.

Table 3: Elemental analysis of oil-prone coal powder

Component	Content range (*w*/%)	Average value (*w*/%)
C	61.78–82.41	72.54
H	4.50–6.12	5.35
N	0.91–3.78	1.28
S	0.58–1.10	0.81
O	8.29–16.77	12.94

2.1.2 Preparation of LaNaY catalyst with the ion exchange method

The preparation process of the LaNaY catalyst is shown in **Figure 1**. The NaY molecular sieve is placed in a box furnace and activated by calcination at 550 °C for 4 h to remove adsorbed water and organic impurities, ensuring the activation of the molecular sieve skeleton. Subsequently, the LaNaY catalyst is prepared using the ion exchange method. A 0.3 mol L^{-1} mixed solution of $La(NO_3)_3$ and $NaNO_3$ is prepared in a predetermined molar ratio (initially 1 : 1). The pH of the solution is adjusted to 5.5 with dilute nitric acid to avoid La^{3+} hydrolysis precipitation and promote ion exchange. The calcined NaY molecular sieve is added to the mixed solution with a solid-liquid ratio of 1 g:20 mL. It is stirred in a water bath at 80 °C for 6 h and the exchange is repeated 3 times to achieve a higher ion exchange degree. After each exchange, it is separated by centrifugation (GL21M high-speed floor centrifuge) and washed repeatedly with deionized water until no white precipitate is detected by $AgNO_3$ in the washing solution (indicating that NO^{3-} has been basically removed). Subsequently, it is washed twice with anhydrous ethanol to reduce pore collapse during drying.[5] Finally, the sample is kept at 110 °C for 12 h for low-temperature slow drying to maintain the structural stability of the molecular sieve. After drying, the sample is placed in a box furnace for secondary roasting. The program is set to raise the temperature to 550 °C at a rate of 2 °C min^{-1} and maintain it for 4 h. This slow heating process helps to avoid metal ion migration and aggregation, ensuring high dispersion of La and Na in the molecular sieve. It is calcined in an air atmosphere to ensure complete decomposition of organic matter.[6] The final product is ground and sieved through a 200 mesh sieve (approximately 75 μm) to ensure particle uniformity and avoid diffusion limiting effects during catalytic experiments. The final product is sealed and stored in a dryer for future use. The concentration of La/Na in the filtrate is determined by ICP-OES (iCAP 7400) to ensure that the target load meets the standard.[7]

2.1.3 Optimization experiment of La loading and pyrolysis temperature

To determine the optimal La loading and pyrolysis temperature of the LaNaY catalyst, gradient experiments are designed in this study.

Optimization of the La loading: Based on the theoretical ion exchange capacity of molecular sieves, LaNaY catalysts with La loading gradients ranging from 0.5 to 3.0 *w*/% are designed.[8] In the experiment, the Na content is fixed and the La:Na molar ratio is 1:1. The preparation process is the same as in section 2.1.2, carried out by preparing $La(NO_3)_3$ solutions of different concentrations for ion exchange. The obtained catalyst is physically and chemically characterized with X-ray diffraction (XRD) and N_2 BET tests to evaluate its crystallinity, skeleton integrity, specific surface area, pore volume, and pore size distribution.[9,10]

Pyrolysis temperature optimization: After determining the optimal La loading amount (determined through the aforementioned experiments to be 1.5 *w*/%) and La:Na molar ratio (1:1), performance tests are conducted on the LaNaY catalyst at different pyrolysis temperatures (500–800 °C, with an interval of 50 °C). The temperature range is based on the main generation zones of tar and gas during coal pyrolysis: tar is mainly generated in the low-temperature zone of coal macromolecular side chain breakage, while gas is mainly generated in the high-temperature zone of aromatic ring condensation and secondary cracking.[11] The experiment sets up a blank control group (without the catalyst) and a NaY molecular sieve control group, and compares them under the same pyrolysis conditions. Oil-prone coal powder is prepared for experimental samples (ground and sieved to 180 μm, dried at 105 °C for 24 h to remove moisture), and me-

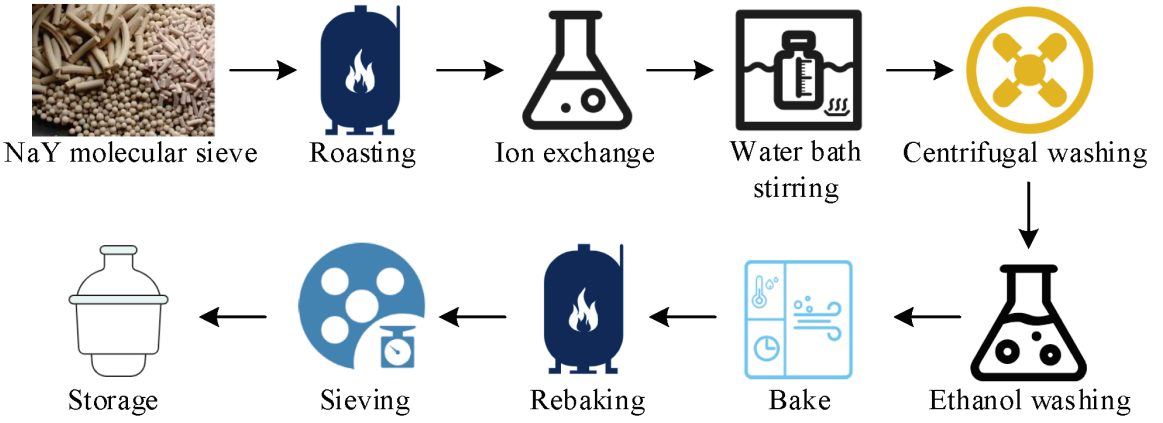

Figure 1: Preparation of LaNaY catalyst

chanically mixed with the optimized 1.5 *w*/% LaNaY catalyst to ensure uniformity. The industrial analysis data in **Table 2** correspond to the coal sample on an žas-received' basis, prior to the drying procedure.

2.2 Control of pyrolysis process parameters

2.2.1 Coal pyrolysis experiment

This experiment uses a laboratory-made fixed-bed pyrolysis reactor (as shown in **Figure 2**). Before reaction, the airtightness of the equipment needs to be checked: all valves are closed, N_2 is introduced to 0.3 MPa, and the pressure is maintained for 10 min. A pressure drop of less than 0.01 MPa min^{-1} is considered qualified.[12] The N_2 mass flow meter is calibrated using a soap film flow meter (50 mL min^{-1}) to ensure an error of less than 2.0 %.[13]

Experimental procedure: The N_2 steel cylinder is opened, the mass flow meter is adjusted to 50 mL min^{-1}, and blowing is continued for 10 min to remove air from the reactor. The glass condenser is filled with 0 °C circulating coolant (ethylene glycol water mixture) and connected to two-stage cold traps at 0 °C and -20 °C to efficiently collect the condensate.[14] The electric heating furnace heats up to the target temperature at a rate of 10 °C min^{-1} and maintains stability through a proportional-integral-derivative (PID) temperature control system, with thermocouples tightly attached to the outer wall of the reaction zone. After reaching the target temperature, the timing of 30 minutes is started and synchronously online GC for gas component analysis is started.[15] The condenser liquefies the pyrolysis vapor and collects the condensate in a pre-weighed glass bottle. The pipeline is rinsed with dichloromethane to ensure complete collection of tar. The online GC collects data every 5 min, with a thermal conductivity detector (TCD) used to detect H_2, CO, CO_2, and a flame ionization detector (FID) used to detect CH_4. The yield of various gases is calculated using integration.[16] After the reaction is complete, the sample is cooled to room temperature under the N_2 protection, semi-coke is taken out and weighed, it is sealed and stored for subsequent characterization.

2.2.2 Rapid pyrolysis experiment of hydrogen

To verify the hydrogenation modification effect of the LaNaY catalyst on tar under the H_2 atmosphere and its protective effect on the active sites of the catalyst, this study compares the pyrolysis experiments under N_2 and H_2 atmospheres. The experimental conditions are set at a reaction temperature of 700 °C, with N_2 and H_2 gas atmospheres selected, and a flow rate of 50 mL min^{-1}. The LaNaY catalyst is used with 1.5 *w*/% La loading and a standardized coal sample, with a reaction time of 20 min.

Leak detection is performed on the fixed-bed reactor before the experiment begins. The quartz tube is filled with a 1:10 mixture of coal and LaNaY, and both ends are fixed with quartz wool. The condensation system is pre-cooled to 0 °C and connected to two-stage cold traps at 0 °C and –20 °C. The N_2 group is purged with 50 mL min^{-1} N_2 for 10 minutes to eliminate air. The H_2 group is first purged with N_2 (50 mL min^{-1}, 10 min), and then switched to an H_2 atmosphere (50 mL min^{-1}) to avoid explosive mixtures. The reactor is heated to 700 °C at a rate of 10 °C min^{-1} and timed for 20 minutes. The online GC collects gas-product data such as $H_2/CH_4/CO/CO_2$ every 2 min, while tar is collected throughout the process. When the reaction is complete, the instrument is turned off and the carrier gas keeps flowing until the temperature drops to room temperature. Finally, semi-coke and catalyst samples are collected.[6,17]

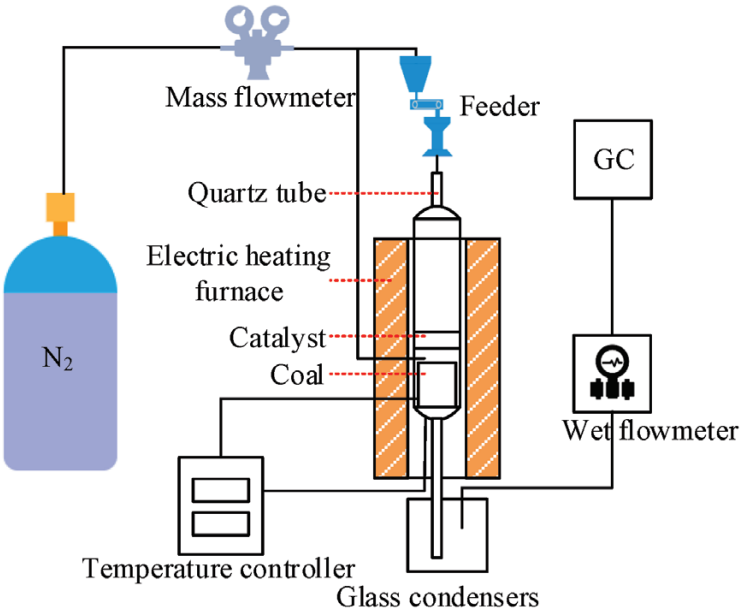

Figure 2: Fixed-bed pyrolysis reactor

2.2.3 Catalyst-coal contact method

To analyze the influence of the contact between the catalyst and coal sample on the selectivity of coal pyrolysis products, this study compares two methods: physical mixing and in-situ loading. The fixed experimental conditions are a flow rate of 50 mL min^{-1} in N_2, a reaction time of 20 min, and a catalyst/coal mass ratio of 1:10.

Physical mixing: 180 μm coal powder is mechanically mixed with 1.5 *w*/% LaNaY catalyst and milled in a ball mill for 10 minutes (at a speed of 300 rpm) to ensure uniformity.[18]

In-situ loading: Coal powder is immersed in a mixed solution of $La(NO_3)_3$ and $NaNO_3$ (La:Na molar ratio 1:1), dried at 80 °C, and calcined at 550 °C for 4 h.[19] This method aims to achieve a more uniform dispersion and loading of LaNaY catalyst components into the coal pore structure. The pyrolysis test temperature is set at 600 °C and 750 °C. The distribution of catalyst on the coal surface is observed and analyzed using SEM and EDS.

2.3 Analysis and characterization of coal pyrolysis products

2.3.1 Coal pyrolysis activity test

To investigate the directional improvement effect of the LaNaY catalyst on the yield of light tar, especially its mechanism of cracking or inhibiting the PAHs,[20,21] the experiment compares three groups: blank coal, NaY molecular sieve, and LaNaY. The fixed reaction temperature is 600 °C, the flow rate is 50 mL min^{-1} in the N_2 atmosphere, the reaction time is 20 min, and the catalyst/coal mass ratio is 1:10. Tar components are analyzed by GC-MS to determine the elements of PAHs such as naphthalene (2-cyclic), phenanthrene (3-cyclic), and pyrene (4-cyclic), and calculate the light/heavy tar ratio.[22]

2.3.2 Gas-product analysis

The gas products are monitored in real-time and analyzed for composition using online GC. H_2, CO, CO_2 are detected by TCD, and CH_4 is detected by FID. The yield is calculated by integrating the peak areas after calibration with standard gas. This study focuses on the yield and selectivity of high-value-added gases such as H_2 and CH_4.

2.3.3 Semi-coke characterization

The property analysis of semi-coke, as a solid product in the pyrolysis process, is of great significance for understanding the pyrolysis mechanism and potential applications. The semi-coke sample is subjected to BET testing for specific surface area and pore-size distribution to evaluate its pore structure. FTIR is used to determine the content of oxygen-containing functional groups such as carboxyl and phenolic hydroxyl groups on the surface of semi-coke, which can affect the subsequent modification of semi-coke.

2.3.4 Tar-composition analysis

The elemental composition (C, H, N, S) of the collected tar is determined using a vario EL cube elemental analyzer, from which the H/C atomic ratio is calculated.

2.4 Theoretical calculation details

To further support the mechanistic discussion, density functional theory (DFT) calculations were performed to compare the adsorption energies of phenanthrene on La^{3+} and Na^{+}. All calculations were conducted using the Gaussian 16 software package. The geometry of phenanthrene and the metal ion-phenanthrene complexes were optimized using the B3LYP density functional. The 6-31G basis set was employed for carbon and hydrogen atoms, while the LANL2DZ effective core potential and basis set were used for La^{3+} and Na^{+}. A cluster model was used to represent the active site, and adsorption energies were calculated by subtracting the energies of the isolated phenanthrene molecule and metal ion from the total energy of the optimized complex.

3 RESULTS AND DISCUSSION

Structural characteristics analysis of LaNaY catalyst

To investigate the structural characteristics of the LaNaY catalyst, this study characterizes the prepared catalyst with XRD, BET, and NH3-TPD. Figure 3 shows characterization results for different catalysts.

From the XRD spectrum in **Figure 3a**, the characteristic diffraction peaks of the NaY molecular sieve appeared at 2θ of 6.05°, 16.35°, and 24.91° for blank NaY, LaNaY, and other comparison catalysts, indicating that the skeleton structure of the molecular sieve was preserved during the ion exchange process. In the XRD spectrum of the LaNaY catalyst, characteristic impurity peaks of La_2O_3 were observed in 20–30° (such as 2θ = 28.5°), indicating that some La^{3+} ions may exist in the form of oxides on the surface or entrance of the molecular sieve during the preparation process. The remaining La^{3+} ions may exist in a highly dispersed form in the molecular sieve pores or successfully enter the molecular sieve skeleton, without significantly changing the phase structure of the molecular sieve. According to the N_2 adsorption-desorption isotherm in **Figure 3b**, the adsorption-desorption isotherms of both LaNaY and NaY exhibit Type I, which is consistent with the characteristics of microporous materials. At a relative pressure of P/P_0 = 0.5, LaNaY exhibits a significant hysteresis curve, indicating the mesoporous structures in LaNaY, which may be attributed to the changes in the pore microstructure after introducing La or the formed La_2O_3 particles. According to the NH3-TPD spectrum in **Figure 3c**, both LaNaY and NaY exhibit two NH3 desorption peaks, corresponding to weak acid sites (100–200 °C) and medium strong acid sites (200–400 °C), respectively.

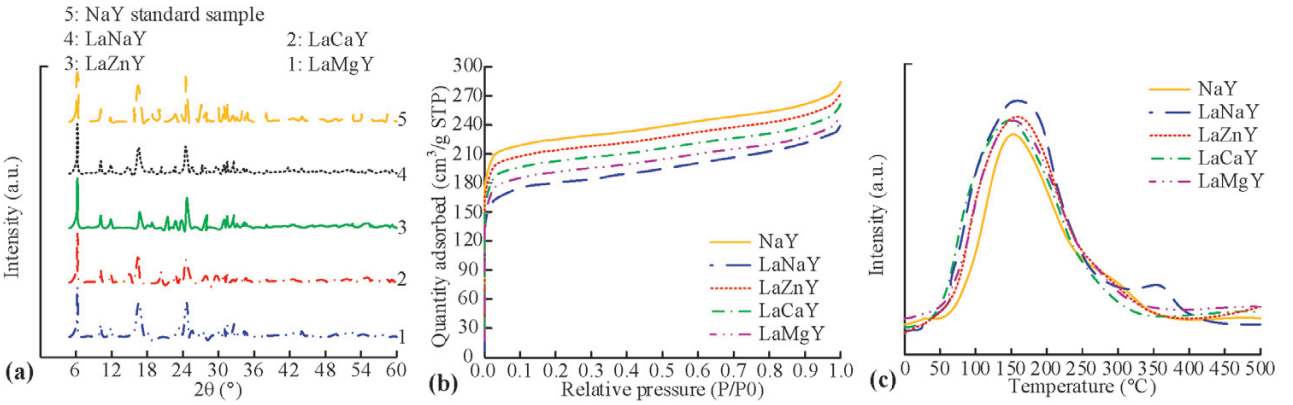

Figure 3: a) XRD spectrum, b) BET test results and c) NH3-TPD characterization results for different catalysts

Compared with the NaY molecular sieve, after introducing the La element, both weak acid content and medium-strong acid content of LaNaY increased, indicating that the Lewis acidity of La^{3+} enhanced the overall acidity of the catalyst. The specific surface area of the parent NaY zeolite is about 896.45 $m^2\ g^{-1}$, with an average pore size of 1.458 nm. The specific surface area of LaNaY slightly decreases to about 848.14 $m^2\ g^{-1}$, but the average pore size slightly increases to 1.525 nm. This indicates that the La and Na metal ions in the pores of the molecular sieve may block some of the micropores, but may also enlarge some of the pores, forming a mesoporous structure that affects the mass transfer and catalytic reactions.

3.2 Analysis of factors affecting LaNaY catalytic performance

3.2.1 Influence of pyrolysis temperature on catalytic performance

The effect of different temperatures on the catalytic activity of LaNaY was investigated under a La loading of 1.5 *w*/% and H_2. The results are shown in **Table 4**. The tar yield increased steadily from 15.2 % at 500 °C to a distinct peak of 18.6 % at 600 °C. The fine temperature gradient confirms that 600 °C is the optimal temperature for maximizing tar production. This indicates that at lower temperatures, the LaNaY catalyst can effectively inhibit the secondary cracking of tar, thereby retaining large molecule tar and increasing its yield. Beyond 600 °C, a further increase in temperature led to a progressive decline in the tar yield, which dropped to 8.9 % at 800 °C. This decrease was accompanied by a significant rise in the gas yield (from 210 mL g^{-1} at 600 °C to 480 mL g^{-1} at 800 °C) and a steady reduction in the semi-coke yield. High temperature promotes deep cracking of tar, converting it into gas products and facilitating the devolatilization of coal. The H_2/CO molar ratio significantly increased within a range of 700–800 °C. For example, the H_2/CO molar ratio reached 2.5 at 700 °C and 3.1 at 800 °C. This indicates that the LaNaY catalyst can significantly promote the water gas shift reaction (if water vapor is present) or the hydrogenolysis reaction of tar/semi-coke at high temperatures, thereby increasing the yield of H_2. It is also plausible that at these higher temperatures, trace residual moisture from the pre-dried coal or oxygen from the coal's structure could participate in the water-gas shift reaction ($CO + H_2O \rightleftharpoons CO_2 + H_2$), which would also contribute to the observed increase in the H_2/CO ratio.

3.2.2 Influence of La loading on catalytic performance

The effects of different La loadings on the tar yield, H_2 selectivity, and specific surface area are shown in **Table 5**. When the La loading was 1.5 *w*/%, both tar yield (18.6 %) and H_2 selectivity (48.3 %) reached their maximum values. When the La loading increased from 0.5 *w*/% to 1.5 *w*/%, the specific surface area decreased from 680 $m^2\ g^{-1}$ to 580 $m^2\ g^{-1}$. Although the specific surface area decreased, it was still greater than 500 $m^2\ g^{-1}$, indicating that its impact on mass transfer is not significant. When the La loading further increased to 3.0 *w*/%, the tar yield and H_2 selectivity decreased, while the specific surface area also further decreased. This may have been due to excessive La loading causing metal particles to agglomerate or block the pores of the molecular sieve, thereby reducing the accessibility of active sites and cat-

Table 4: Quantitative relationship between different temperatures and LaNaY catalytic activity

Temperature (°C)	500	550	575	600	625	650	700	750	800
Tar yield (%)	15.2	16.8	18.1	18.6	17.1	15.5	12.4	10.3	8.9
Gas yield (mL g^{-1})	120	165	185	210	245	280	350	415	480
Semi-coke yield (%)	72.1	68.9	67.1	65.3	63.7	62.0	58.7	55.2	52.0
H_2/CO molar ratio	0.8	1.0	1.1	1.2	1.5	1.8	2.5	2.8	3.1

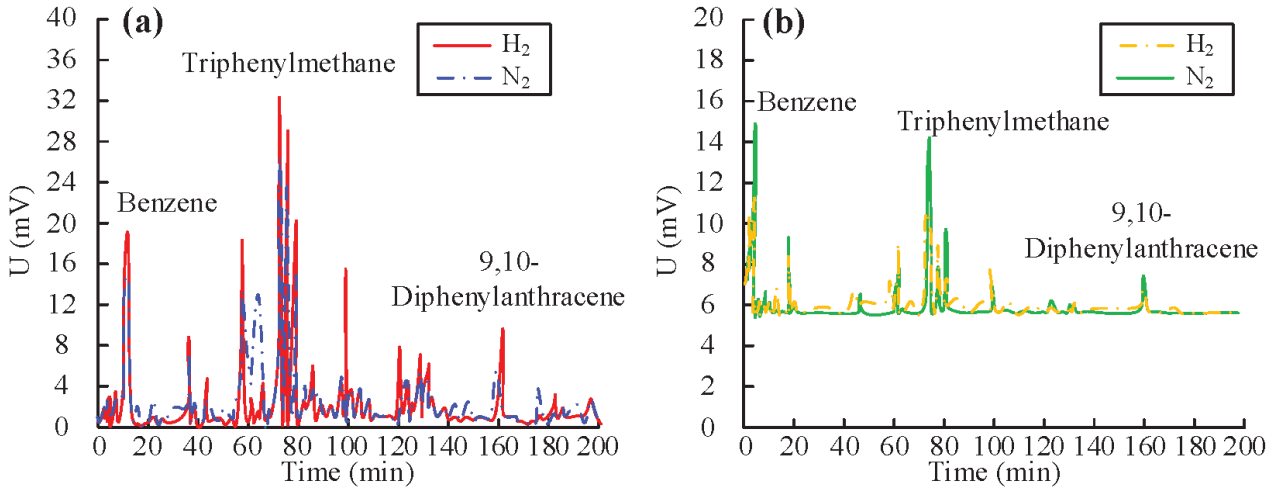

Figure 4: GC-MS analysis results for: a) light aromatic hydrocarbons, b) heavy PAHs

alytic efficiency. Considering both performance and economy, the optimal La loading is 1.5 *w*/%.

Table 5: Performance results for different La loadings

La load capacity (*w*/%)	Tar yield (%)	H_2 selectivity (%)	Specific surface area ($m^2\ g^{-1}$)
0.5	12.3	35.2	680
1.0	15.4	41.5	620
1.5	18.6	48.3	580
2.0	16.2	45.1	520
3.0	13.8	39.7	450

3.2.3 Influence of H_2 atmosphere on product distribution

Figure 4 shows the GC-MS analysis results for the effect of the H_2 atmosphere on the content of light aromatic hydrocarbons and heavy PAHs in tar. According to **Figure 4a**, compared to the N_2 atmosphere, the content of light components in tar significantly increased under the H_2 atmosphere, with benzene increasing by 20 %. This confirms that H_2 has a promoting effect on the generation of light aromatic hydrocarbons, which may be achieved through hydrocracking or inhibiting polymerization reactions. According to **Figure 4b**, the H/C atomic ratio of H_2 tar increased from 1.2 to 1.5, while the content of heavy PAHs decreased by 50 %. This indicates that the reduction of H_2 promotes hydrogenation degradation or conversion of heavy PAHs into lighter components, effectively optimizing the tar quality and reducing harmful components.

Figure 5 further illustrates the variations in tar, gas, and semi-coke yields with temperature under different atmospheres. In **Figure 5a**, the tar yield under the H_2 atmosphere is higher than that under the N_2 atmosphere at 400–600 °C, reaching its maximum value at 600 °C (18.6 % vs 16.9 %). In **Figure 5b**, the gas yield in the H_2 atmosphere is consistently higher than that in the N_2 atmosphere within a range of 500–700 °C, which is consistent with the conclusion that the H_2 atmosphere promotes gas generation (such as H_2 and CH_4). In **Figure 5c**, the decrease rate in the yield of semi-coke under the H_2 atmosphere is faster than that under the N_2 atmosphere, especially in a range of 430–700 °C, indicating that H_2 could promote further conversion of semi-coke.

3.2.4 Influence of catalyst-coal contact mode

Figure 6 shows the SEM-EDS results for La on the coal surface under two contact modes: physical mixing and in-situ loading. In **Figure 6a**, the distribution of La in the sample prepared by physical mixing is uneven, with a coefficient of variation (CV) as high as 35 %, which may lead to local overheating and damage to the

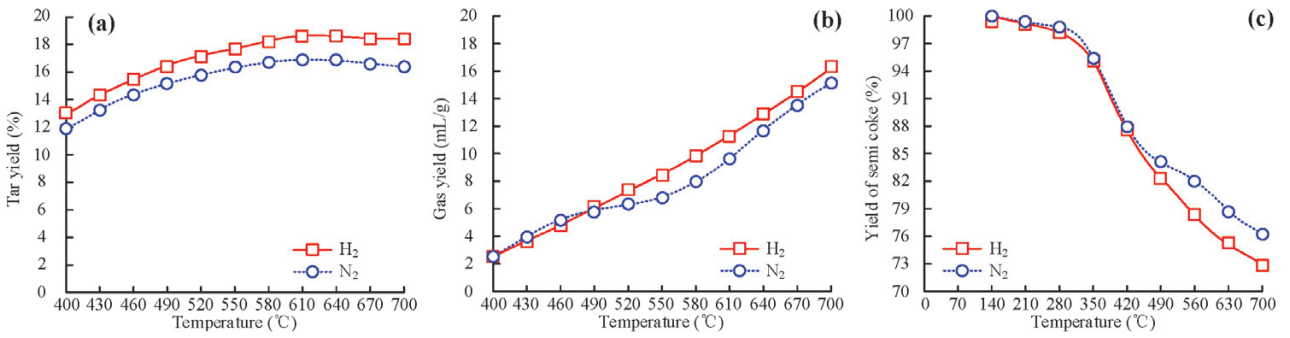

Figure 5: Yield results for: a) tar, b) gas and c) semi-coke coal pyrolysis products influenced by different gases

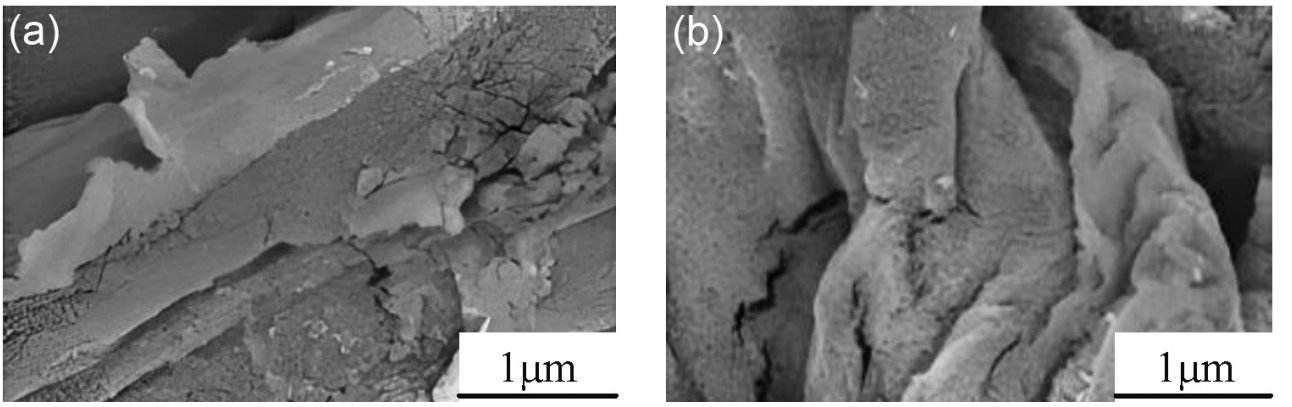

Figure 6: SEM-EDS results for La on the coal surface under: a) physical mixing and b) in-situ loading contact modes

catalyst structure. In **Figure 6b**, under in-situ loading, the distribution of La is more uniform, the CV value of the EDS surface scan is less than 15 %, and the overlap between La and coal pores exceeds 80 %. The in-situ loaded sample retains more 2–10 nm mesopores. This indicates that in-situ loading can disperse the La element more uniformly in the microstructure of coal, thereby enabling a more effective distribution of catalytic active sites and sufficient contact with coal components, significantly improving catalytic efficiency.

Table 6 compares the effects of different contact methods and temperatures on the coal pyrolysis product distribution. At 600 °C, in-situ loading of LaNaY resulted in a tar yield of 18.6 %, significantly higher than that of physical mixing (16.2 %). This is due to a more optimized catalyst coal interface contact, where the active centers can more effectively promote tar generation. At 600 °C, in-situ loading increased the proportion of light aromatic hydrocarbons in tar from 45 % under physical mixture to 58 %, with an increase of 13 %. This indicates that in-situ loading is more conducive to the aromatization reaction of tar and optimizes its quality. At 750 °C, in-situ loading facilitated a gas-phase cracking reaction and H_2 generation, with the H_2 yield reaching 280 mL g^{-1}, which was 33 % higher than under physical mixing. Meanwhile, under in-situ loading, the selectivity of CH_4 was 18 %, which was 7 % lower than that under physical mixing, indicating that it promotes deep cracking of small molecule gases and is beneficial for improving the H_2 selectivity. Overall, compared with physical mixing, in-situ loading at 600 °C produces higher tar and H_2 yields, and reduces methane generation, making this method more suitable for coal pyrolysis processes that require high H_2 production.

Table 6: Influence of different contact methods on product distribution

Temperature (°C)	600		750	
Contact method	Tar yield (%)	Proportion of light aromatic hydrocarbons (%)	H_2 yield (mL g^{-1})	CH_4 selectivity (%)
Physical mixing	16.2	45	210	25
In-situ loading	18.6	58	280	18

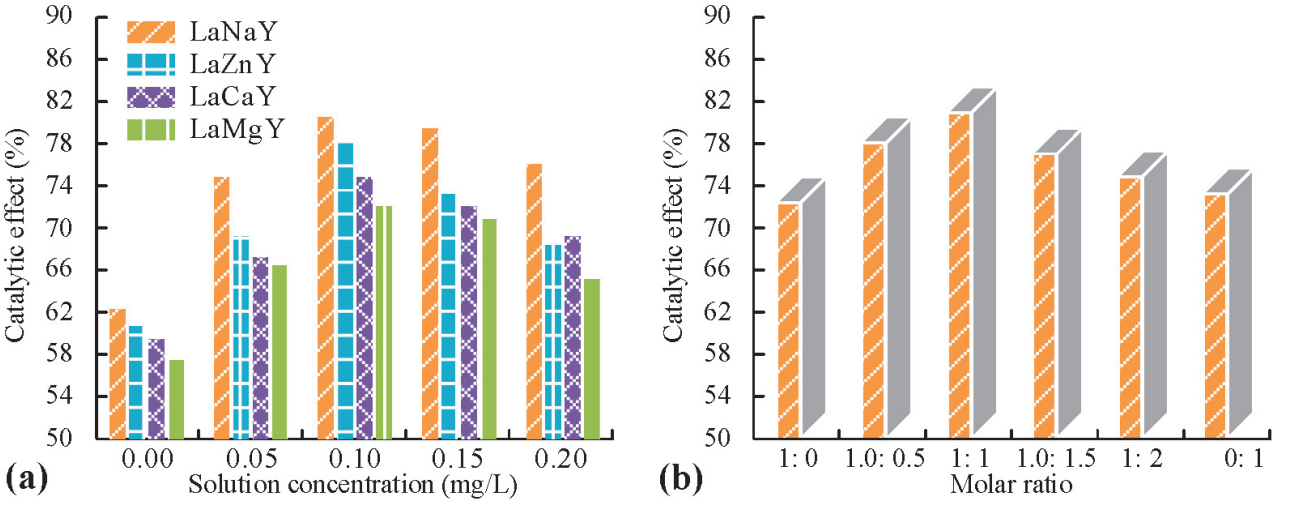

Figure 7: Effects of different: a) metal solution concentrations and b) La:Na molar ratios on the pyrolysis performance of LaNaY catalyst

3.3 Performance analysis and mechanism exploration of LaNaY catalyst

3.3.1 Influence of preparation conditions for LaNaY catalyst on pyrolysis performance

This study also investigated the effects of different metal solution concentrations and La:Na molar ratios on the pyrolysis performance of the LaNaY catalyst (as shown in **Figure 7**). In **Figure 7a**, where the concentration of $La(NO_3)_3$ and $NaNO_3$ mixed solution is 0.1 mol L^{-1}, the tar yield of LaNaY reaches its highest and the catalytic effect is significant. This indicates that increasing the concentration of metal ions within a certain range can increase the active sites of the catalyst, thereby improving catalytic efficiency. However, when the concentration of the solution is too high, it may cause blockage of the molecular sieve pores due to excessive metal ions, reducing the specific surface area and the number of active centers in the molecular sieve, thereby weakening the catalytic effect. In **Figure 7b**, at a constant solution concentration, as the molar amount of La decreases and the molar amount of Na increases, the tar yield of the catalyst shows an initial increase followed by a slow decrease. This may be due to the lower single metal ion exchange capacity of La or Na, while increasing the amount of another metal ion appropriately can increase the selectivity and activity of the catalyst. La_2O_3 and NaO may have a synergistic effect, enhancing the catalytic ability. Therefore, the suitable La/Na molar ratio for the LaNaY catalyst is 1:1.

3.3.2 Optimization of tar components and mechanism exploration

Table 7 presents the contents of benzene, naphthalene, and phenanthrene in the pyrolysis products of blank coal, NaY, and LaNaY catalysts, as well as their light-to-heavy weight ratios. Compared with blank coal and NaY, the LaNaY group had the highest benzene content (2100 μg g^{-1}), while the naphthalene (480 μg g^{-1}) and phenanthrene (220 μg g^{-1}) had the lowest content. The light-to-heavy weight ratio significantly increased from 1.41 for blank coal and 1.89 for NaY to 3.75 for LaNaY. This clearly indicates that the LaNaY catalyst can generate more light aromatic hydrocarbons during pyrolysis and effectively suppress the generation of heavy PAHs such as naphthalene and phenanthrene.

Table 7: Distribution of tar components

Group	Blank coal	NaY	LaNaY
Benzene (μg g^{-1})	1200	1450	2100
Naphthalene (μg g^{-1})	850	720	480
Phenanthrene (μg g^{-1})	420	380	220
Light-to-heavy ratio	1.41	1.89	3.75

This selective improvement is attributed to the specific adsorption and directed cleavage of PAHs by the LaNaY catalyst. La^{3+} has strong Lewis acidity and preferentially adsorbs planar structures of PAHs (such as phenyl rings in phenanthrene) through π-complexation, inhibiting their condensation in the gas phase. This type of cation-π interaction is a fundamental, well-documented noncovalent force driven primarily by electrostatics.[23,24] The strength of this interaction is known to be highly dependent on the charge density of the cation, with divalent cations like Mg^{2+} exhibiting much stronger binding to π-systems than monovalent cations.[25,26] Therefore, the trivalent La^{3+} ion, possessing a very high charge density, is expected to engage in a particularly strong electrostatic interaction with the electron-rich π-systems of PAHs, which supports its role in selectively adsorbing these molecules and altering their reaction pathways. The relevant reaction is shown in Equation (1).[27]

$$PAH + La^{3+} \rightarrow PAH\text{-}La^{3+}_{ads} \quad (1)$$

In Equation (1), La^{3+} interacts with the π electrons of aromatic rings in PAHs to form surface adsorption complexes. La^{3+} preferentially adsorbs planar PAHs (such as phenanthrene) rather than fatty chains, inhibiting random cracking.[28] This study uses the density functional theory (DFT) to calculate the adsorption energy between La^{3+} and phenanthrene molecules. The calculation results showed that the adsorption energy of La^{3+} for phenanthrene (–2.3 eV) was significantly higher than that of Na^+ (–1.5 eV), strongly confirming that LaNaY has a stronger ability to selectively adsorb aromatic ring structures of PAHs.

Furthermore, under an H_2 atmosphere, the LaNaY catalyst significantly promotes the formation of light aromatics. We propose that this occurs through the activation of H_2 on the catalyst surface, followed by the hydrogenolysis of heavy PAHs. As illustrated in **Figure 8**, the mechanism is likely initiated by the heterolytic dissociation of the H_2 molecule. This process is a cooperative effort between the Lewis acidic La^{3+} site and a neighboring Lewis basic-framework oxygen atom of the Y-zeolite, an interaction model supported by reports of strong bonding between La and the framework oxygen atoms in Y-zeolites.[29] The H-H bond is cleaved unevenly, forming a hydride ion (H^-) stabilized by the La^{3+} center (forming La-H) and a proton (H^+) that binds to the framework oxygen, creating a Brønsted acid site (O-H). The proposed generation of new Brønsted acid sites is consistent with the experimental finding that La incorporation increases the Brønsted acidity of Y-zeolites.[29] These two highly reactive surface hydrogen species are then available to attack and cleave the C-C bonds of adsorbed PAHs. This overall capability for H_2 activation and subsequent reaction is in agreement with the established role of La-modified zeolites in promoting hydrogenation and hydrogen transfer reactions in processes such as hydrocracking.[29,30] It should be noted that while this proposed mechanism provides a chemically sound explanation for our observations, its definitive confirmation would require further dedicated mechanistic studies, such as H_2-TPD or isotope labeling experiments.

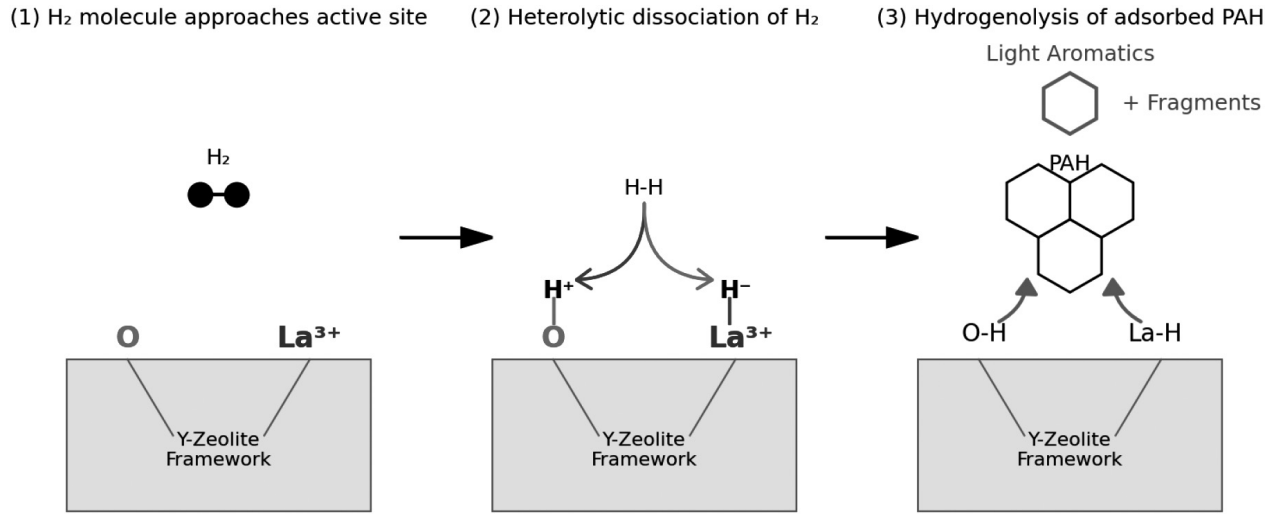

Figure 8: Proposed mechanism for the activation of H_2 on the LaNaY catalyst surface via heterolytic dissociation

The relevant reaction is shown in Equation (2).[31]

$$\text{Pyrene(4-ring)} + 5H_2 \xrightarrow{\text{LaNaY}} 2\text{Toluene} + 2CH_4 \quad (2)$$

Lewis acid sites can also activate weak C-C bonds in PAHs (such as the 9,10 positions of anthracene), further promoting their cleavage. The relevant reaction is shown in Equation (3).

$$PAH\text{-}La^{3+}_{(ads)} + H_2O \rightarrow \text{Lighter aromatics} + CO + H_2 \quad (3)$$

3.3.3 Mechanism for the increase in rich gas production

The LaNaY catalyst can not only optimize tar products, but also generate high-value-added gases. When the pyrolysis temperature was increased to 700 °C or 750 °C, the gas yield significantly increased (as shown in **Tables 2** and **4**), and the H_2/CO molar ratio also increased significantly. This indicates that the LaNaY catalyst can reduce the reaction energy barrier, promoting the secondary cracking of tar/semi-coke and potentially the coal gasification reaction in the presence of water vapor, thereby increasing the yield of high-value-added gases such as H_2 and CH_4.

3.3.4 Catalyst stability, deactivation, and reusability

The long-term stability and reusability of a catalyst are critical for its industrial applicability. Therefore, a recycling experiment was conducted to evaluate the performance of the LaNaY catalyst over five consecutive pyrolysis cycles. Furthermore, to probe the deactivation mechanism as suggested by the reviewer, the coke content on the spent catalyst after each cycle was quantified using thermogravimetric analysis (TGA).

The results are presented in **Figure 9**. As shown by the blue bars (left axis), the catalyst exhibited good stability. The tar yield gradually decreased from 18.6 % in the first run to 16.6 % in the fifth run. To understand the cause of this deactivation, the amount of deposited coke was tracked, as shown by the red line (right axis). The coke content steadily increased from 2.5 *w*/% after the first cycle to 10.5 *w*/% after the fifth. This strong inverse

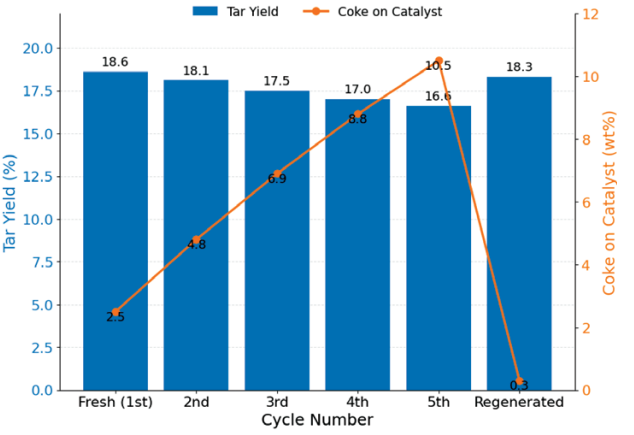

Figure 9: Recycling performance (blue bars, left axis) and coke deposition (red line, right axis) of the LaNaY catalyst (reaction conditions: T = 600 °C, H_2 atmosphere, catalyst/coal ratio = 1:10; regeneration: calcination in air at 550 °C for 4 h)

correlation convincingly demonstrates that the gradual deactivation is primarily caused by the accumulation of coke on the catalyst's active sites and within its pores.

To investigate its potential for regeneration, the catalyst used in the fifth run was regenerated by calcination in air. As shown in the final data point, the regeneration was highly effective. The tar yield was restored to 18.3 %, recovering 98.4 % of the initial activity. Concurrently, the coke content was reduced to a negligible 0.3 *w*/%. These findings demonstrate that the deactivation is largely reversible and that the LaNaY catalyst possesses excellent structural stability and regeneration potential, making it a highly promising candidate for practical applications.

4 CONCLUSION

This study successfully prepared a LaNaY catalyst using ion exchange method and systematically investi-

gated its effect on product distribution during the pyrolysis of oil-prone coal. The research results indicate that:

1. The LaNaY catalyst exhibited the best catalytic performance when La loading was 1.5 *w*/%, the La:Na molar ratio was 1:1, and in-situ loading was used.

2. Under a pyrolysis temperature of 600 °C, H_2 atmosphere, and in-situ loading conditions, the tar yield reached its maximum value of 18.6 %. The H_2 atmosphere significantly increased the generated light aromatic hydrocarbons in tar, and the H/C atomic ratio of tar from 1.2 to 1.5. In addition, the content of heavy PAHs decreased by 50 %, effectively improving the quality of tar.

3. The catalyst's mechanism for upgrading tar involved a dual function: its enhanced Lewis acidity promoted the selective adsorption of heavy PAHs via π-complexation, inhibiting coke formation, while under an H_2 atmosphere, it facilitated the heterolytic dissociation of H_2 to generate active hydrogen species, crucial for the hydrogenolysis of heavy molecules into light aromatics.

4. At a higher pyrolysis temperature (700 °C), the LaNaY catalyst significantly promoted the generation of gas products, especially in the H_2 atmosphere, where the H_2/CO molar ratio reached 2.5, highlighting its potential for producing high-value-added syngas or hydrogen-rich gas products.

5. The LaNaY catalyst demonstrated excellent operational stability and reusability over five consecutive pyrolysis cycles. Deactivation was primarily caused by reversible coke deposition, and the catalyst's initial high activity was almost fully recovered after a simple regeneration process, confirming its robustness and potential for practical applications.

In summary, the LaNaY catalyst can effectively improve the tar yield, enhance the tar quality, and optimize gas product distribution. The study provides an effective solution for an efficient and high-value conversion of oil-prone coal, which is of great significance for coal pyrolysis optimization and the green development of the coal chemical industry. Future work should focus on the long-term stability, deactivation mechanism, and applicability of the LaNaY catalyst to different coal types. A more comprehensive analysis of all gaseous products, including valuable C_2-C_4 hydrocarbons, should be carried out to fully assess its potential for generating high-value chemicals. A combination of these studies with in-situ characterization techniques will allow for a thorough analysis of its catalytic conversion pathway at the molecular level.

Acknowledgment

This work was supported by the project Research on Key Technologies for Hydrogen-Assisted Rapid Pyrolysis of 100,000 Tons per Year Oil Rich Coal (Grant No. 2024A01007-3), and the Hami Oil-Rich Coal Clean and Efficient Use Innovation Team (Grant No. 2024hmkjcxtd01). The authors gratefully acknowledge the financial support.

5 REFERENCES

[1] W. Kalkreuth, M. Ruaro Peralba, S. Barrionuevo, R. Hinrichs, T. Silva, H. Maman Anzolin, E. Osorio, J. Pohlmann, B. De Caumia, H. Pakdel, C. Roy, Vacuum Pyrolysis of Brazilian coal, peat and biomass – Results on characterization of feedstock, solid residues, pyrolysis liquids and conversion rates, Energ. Explor. Exploit., 42 (**2024**) 3, 817–836, doi:10.1177/01445987231225253

[2] X. An, Y. Zhang, Y. Shang, Y. Tian, Y. Qiao, Study of Pyrolysis Characteristics and Kinetic Analysis of Shenmu Coal at a High Heating Rate Using TG-FTIR, China Pet. Process. Pe. Technol., 26 (**2024**) 1, 47–55

[3] J. Liu, X. Yang, J. Liu, X. Jiang, Microscopic pyrolysis mechanisms of superfine pulverized coal based on TG-FTIR-MS and ReaxFF MD study, Energy, 289 (**2024**), 130031–130033, doi:10.1016/j.energy.2023.130031

[4] H. Merdun, M. Yildirim, Pyrolysis and combustion of industrial hemp, coal and their blends for thermal analysis by thermogravimetric analysis/Fourier transform infrared spectrometer, Waste Manage Res., 43 (**2025**) 2, 192–206, doi:10.1177/0734242X241241604

[5] Y. Jia, Y. Liu, H. Shu, Z. Wang, Y. Wang, S. Li, L. Lin, F. Lian, Catalytic pyrolysis of tar-rich coal for coal tar to light oil with catalysts of modified granulated blast furnace slag, J. Therm. Anal. Calorim., 149 (**2024**) 8, 3097–3110, doi:10.1007/s10973-024-12932-z

[6] C. Ma, S. Kumagai, Y. Saito, T. Yoshioka, X. Huang, Y. Shao, J. Ran, L. Sun, Recent Advancements in Pyrolysis of Halogen-Containing Plastics for Resource Recovery and Halogen Upcycling: A State-of-the-Art Review, Environ. Sci. Technol., 58 (**2024**) 3, 1423–1440, doi:10.1021/acs.est.3c09451

[7] J. Li, K. Zeng, D. Zhong, G. Flamant, A. Nzihou, C. E. White, H. Yang, H. Chen, Algae Pyrolysis in Molten NaOH-Na2CO3 for Hydrogen Production, Environ. Sci. Technol., 57 (**2023**) 16, 6485–6493, doi:10.1021/acs.est.3c01325

[8] W. Meng, B. Xing, S. Cheng, Y. Nie, H. Zeng, X. Qu, B. Xu, C. Zhang, J. Yu, S. W. Hong, Preparation of high quality carbon nanotubes by catalytic pyrolysis of waste plastics using FeNi-based catalyst, Waste Manage., 189 (**2024**), 11–22, doi:10.1016/j.wasman.2024.08.005

[9] E. Sert, E. Y. Mertsoy, M. Sert, Catalytic Production of Glycerol Carbonate from Glycerol Using Sunflower Stalk-Derived Biochars: Fabrication, Characterization, and Performance Evaluation, Catal. Surv. Asia, 29 (**2025**) 2, 127–138, doi:10.1007/s10563-024-09444-z

[10] D. Bissinger, J. H. Honerkamp, J. Roldan, J. Bremes, K. Kannen, M. K. Lake, A. Roppertz, Development of Catalytically Functionalized Polyester-Based Filters Produced by Flame Spray Pyrolysis, Top. Catal., 67 (**2024**), 539–550, doi:10.1007/s11244-023-01892-7

[11] J. Zhang, D. Lai, Z. Chen, X. Wang, Q. Xiong, J. Li, X. Zhang, B. O. Oboirien, G. Xu, CO2-Assisted Catalytic Pyrolysis of Polyolefins to Aromatics over Mesoporous HZSM-5 and Ga/ZSM-5 Catalysts, Acs. Sust. Chem. Eng., 12 (**2024**) 35, 13137–13148, doi:10.1021/acssuschemeng.4c02858

[12] M. Hamdan, L. Halawy, A. Hijazi, S. Aouad, J. Zeaiter, Highly-stable Ni-Zn catalyst on USY zeolite support for low temperature methane pyrolysis, Int. J. Hydrogen Energ., 61 (**2024**), 840–850, doi:10.1016/j.ijhydene.2024.02.370

[13] B. P. Aduev, V. D. Volkov, Pyrolysis of Brown Coal Microparticles under the Action of Nanosecond First-Harmonic Pulses from a Neodymium Laser, B. Lebedev, Phys. Inst., 51 (**2024**) 1, S66–S75, doi:10.3103/S1068335624600116

[14] Q. Liu, B. Peng, N. Cai, Y. Su, S. Wang, P. Wu, Q. Cao, H. Zhang, Simultaneous production of high-valued carbon nanotubes and hydrogen from catalytic pyrolysis of waste plastics: The role of cellu-

lose impurity, Waste Manage., 174 (**2024**), 420–428, doi:10.1016/j.wasman.2023.12.026

[15] X. Guo, Y. Tang, H. H. Schobert, C. F. Eble, C. Chen, Inspired by the Optical Properties of Char and Coke: A Study on Differences between Them from Perspectives of Organic Elemental Contents and the Carbon Nanostructure, Energ. Fuel., 38 (**2024**) 5, 3713–3727, doi:10.1021/acs.energyfuels.3c04621

[16] A. Salimbeni, M. Di Bianca, A. M. Rizzo, D. Chiaramonti, Application of an integrated pyrolysis and chemical leaching process for pulper waste conversion into coal, hydrogen and chemical flocculating agent, Waste Manage., 174 (**2024**), 549–557, doi:10.1016/j.wasman.2023.12.038

[17] H. Zuo, K. Zeng, D. Zhong, J. Li, H. Xu, Y. Lu, W. Lu, H. Zhou, G. Flamant, H. Yang, H. Chen, Design of a Self-Management Solar Pyrolysis Packed-Bed Reactor by Coupling Thermal Energy Storage, Energ. Fuel., 37 (**2023**) 3, 2134–2148, doi:10.1021/acs.energyfuels.2c03884

[18] M. Pan, C. Jin, B. Han, R. Ye, R. Zhang, G. Feng, A theoretical insight about co-pyrolysis reaction of natural gas and coal, Chinese J. Chem. Eng., 63 (**2023**) 11, 220–225, doi:10.1016/j.cjche.2023.05.007

[19] J. Narangerel, A. Ariunaa, O. Nasantogtokh, E. Munkhbat, Hydrotreatment of Middle Distillate from Pyrolysis Tar by Using Fixed Bed Reactor, Solid. Fuel. Chem., 59 (**2025**) 1, 21–26, doi:10.3103/S0361521924700460

[20] T. Das, S. Das, P. Kumar, C. A. Betty, D. Mandal, Coal waste-derived synthesis of yellow oxidized graphene quantum dots with highly specific superoxide dismutase activity: characterization, kinetics, and biological studies, Nanoscale, 15 (**2023**) 44, 17861–17878, doi:10.1039/d3nr04259f

[21] X. Liu, H. Song, K. Han, J. Hu, Z. Zhao, P. Cui, Insight into low-temperature co-pyrolysis of Qinglongshan lean coal with organic matter in Huadian oil shale, Energy, 285 (**2023**), 128678–128679, doi:10.1016/j.energy.2023.128678

[22] J. Wu, Z. Zhang, D. Li, Y. Zhang, J. Wang, J. Jiang, Converting waste tires into p-cymene through hydropyrolysis and selective gas-phase hydrogenation/dehydrogenation, Waste Manage., 174 (**2024**), 282–289, doi:10.1016/j.wasman.2023.12.009

[23] N. Kumar, A. S. Gaur, G. N. Sastry, A perspective on the nature of cation-π interactions, J. Chem. Sci., 133 (**2021**) 4, 97, doi:10.1007/s12039-021-01959-6

[24] D. A. Dougherty, The Cation-π Interaction in Chemistry and Biology, Chem. Rev., 125 (**2025**) 5, 2793–2808, doi:10.1021/acs.chemrev.4c00707

[25] T. Zhou, N. Wang, Y. Gao, X. Li, Cation–π interactions in polymer science: from fundamental insights to material applications, Polym. Chem., 16 (**2025**) 18, 2058–2074, doi:10.1039/D5PY00232J

[26] H. Geng, P. Zhang, Q. Peng, J. Cui, J. Hao, H. Zeng, Principles of cation-π interactions for engineering mussel-inspired functional materials, Acc. Chem. Res., 55 (**2022**) 8, 1171–1182, doi:10.1021/acs.accounts.2c00068

[27] G. Ji, B. Liu, G. Luo, Y. Chao, P. Fang, S. Gong, S. Guo, C. Wang, K. Hou, Research Progress on Gas Generation from Waste Plastics Through Pyrolysis, Korean. J. Chem. Eng., 41 (**2024**) 9, 2477–2493, doi:10.1007/s11814-024-00216-z

[28] Z. Zhang, C. Liu, Q. Deng, S. Li, M. Yao, Experimental and simulation study on the thermal decomposition of Xishan coal and the pyrolysis of coal with Na_2SO_4, Mol. Simulat., 50 (**2024**) 13, 980–990, doi:10.1080/08927022.2024.2375743

[29] S. Yu, J. Yan, W. Lin, J. Long, S. B. Liu, Effects of lanthanum incorporation on stability, acidity and catalytic performance of Y zeolites, Catal. Lett., 151 (**2021**) 3, 698–712, doi:10.1007/s10562-020-03357-y

[30] C. Mendoza, C. Manrique, A. Echavarría, Impact of lanthanum ion exchange and steaming dealumination on middle distillate production using nanosized Y zeolite catalysts in hydrocracking reactions, RSC Adv., 14 (**2024**) 37, 26760–26774, doi:10.1039/D4RA04664A

[31] A. L. Jadhav, P. A. Gardi, P. A. Kadam, Critical Review of Heterogeneous Catalysts: Manufacturing of Fuel from Waste Plastic Pyrolysis, Korean. J. Chem. Eng., 41 (**2024**) 11, 2937–2960, doi:10.1007/s11814-024-00273-4